Pergamon

Int. J. Heat Mass Transfer. Vol. 38, No. 6, pp. 1063–1073, 1995

0017-9310/95 $9.50+0.00

0017-9310(94)00217-7

Natural convection in rectangular enclosures heated from below and symmetrically cooled from the sides

MARCELO M. GANZAROLLI and LUIZ F. MILANEZ

Departamento de Energia, FEM CP 6122, Universidade Estadual de Campinas, 13081-970 Campinas, São Paulo, Brasil

(*Received* 30 *June* 1993 *and in final form* 7 *July* 1994)

Abstract—Steady natural convection in an enclosure heated from below and symmetrically cooled from the sides is studied numerically, using a streamfunction–vorticity formulation. The Allen discretization scheme is adopted and the discretized equations were solved in a line by line basis. The Rayleigh number based on the cavity height is varied from 10^3 to 10^7. Values of 0.7 and 7.0 for the Prandtl number are considered. The aspect ratio L/H (length to height of the enclosure) is varied from 1 to 9. Boundary conditions are uniform wall temperature and uniform heat flux. For the range of the parameters studied, a single cell is observed to represent the flow pattern. Numerical values of the Nusselt number as a function of the Rayleigh number are reported, and the Prandtl number is found to have little influence on the Nusselt number. A scale analysis is presented in order to better understand the phenomenon.

INTRODUCTION

The phenomenon of natural convection in fluid-filled rectangular enclosures has received considerable attention in recent years. This attention is due mainly because this phenomenon often affects the thermal performance in many engineering applications. The present work was motivated by a more general analysis of the heat transfer in electronic equipments.

Natural convection in closed cavities has been studied primarily in fluid layers heated from below or fluid layers heated from the side. Rather little work is carried out regarding more complex boundary conditions such as the case when the imposed gradient is neither horizontal nor vertical, specially for shallow or tall cavities. In a recent review on natural convection in cavities, Ostrach [1] observed that this configuration, which also occurs when the cavity is inclined, can be viewed as an exception among the works on this topic. Kimura and Bejan [2] considered natural convection in a corner region formed by a vertical warm wall rising above a cold horizontal wall. Constant heat flux as well as uniform temperature boundary conditions were used. The problem was solved numerically and a scale analysis predicted the persistence of a single cell. Small values of Rayleigh number expansions indicated that the flow field in this case is relatively insensitive to the nature of the boundary condition. Anderson and Lauriat [3] studied the flow in a cooled square cavity heated from below and cooled from one side. Except for a vertical adiabatic wall, the boundary conditions are the same as that of the cavity in the present study. Numerical calculations and experimental results confirm a single cell flow pattern and the absence of Bénard-type instabilities, despite the unstable vertical temperature gradient adjacent to the heated floor. November and Nansteel [4] studied the natural convection flow in a square enclosure with one cooled vertical wall and the cavity floor partially heated. They observed that the heated layer adjacent to the lower surface remains attached up to the turning corner though the density stratification in this layer is unstable. A question is left whether this layer would remain attached for larger aspect ratio enclosures.

In this work a rectangular enclosure heated from below and symmetrically cooled from the sides is analyzed. The boundary condition for the cavity floor is uniform temperature or uniform heat flux while the side walls are cooled at a uniform temperature. The basic governing equations are solved numerically for rectangular enclosures with the aspect ratio L/H ranging from 1 to 9. Parameters like the Nusselt number and the maximum value of the streamfunction are related to the Rayleigh number, and the influence of the Prandtl number verified. A scale analysis is performed in order to better understand the phenomenon and consequently explain the correlations obtained from numerical results.

MATHEMATICAL FORMULATION

Consider a two-dimensional cavity of height H and length $2L$ completely filled with a Newtonian fluid such as air or water shown in Fig. 1 along with the coordinate system employed. The cavity is symmetrically cooled from the two vertical side walls kept at temperature t_c. The boundary condition at the cavity floor can be of the first or second kind: uniform temperature t_h or uniform positive heat flux q''. Due to

NOMENCLATURE

g	gravitational acceleration
Gr	Grashof number, Ra/Pr
H	cavity height
k	thermal conductivity
l	thermal penetration length
L	cavity half length
Nu	Nusselt number
Pr	Prandtl number, v/α
q''	heat flux
Q	overall heat transfer rate
Ra	Rayleigh number, $g\beta H^3(t_h-t_c)/v\alpha$ or $g\beta H^4 q''/v\alpha k$
t	temperature
$\bar{t}_h$	cavity floor average temperature
Δt	temperature difference, (t_h-t_c)
T	dimensionless temperature, $(t-t_c)/(t_h-t_c)$ or $(t-t_c)/(q''H/k)$
u	horizontal velocity component
U	dimensionless horizontal velocity component, uH/α
v	vertical velocity component
V	dimensionless vertical velocity component, vH/α
x	horizontal coordinate
X	dimensionless horizontal coordinate, x/H
y	vertical coordinate
Y	dimensionless vertical coordinate, y/H.

Greek symbols

α	thermal diffusivity
β	coefficient of thermal expansion
δ	boundary layer thickness
δ_t	thermal boundary layer thickness
v	kinematic viscosity
ξ'	vorticity
ξ	dimensionless vorticity, $\xi' H^2/\alpha$
ϕ	generalized dimensionless variable (ξ or T)
ψ'	streamfunction
ψ	dimensionless streamfunction, ψ'/α.

Subscripts

c	cold surface
h	hot surface.

the symmetry of the problem only half of the enclosure has to be considered. Laminar and two-dimensional flow is assumed and the usual Boussinesq approximation for the governing equations is adopted. It is convenient to deal with the equations and boundary conditions in dimensionless form. Selecting reference quantities for length, velocity and temperature, the following group of dimensionless variables can be defined as

$$X=\frac{x}{H} \quad Y=\frac{y}{H}$$
$$U=\frac{u}{(\alpha/H)} \quad V=\frac{v}{(\alpha/H)}$$
$$T=\frac{t-t_c}{t_h-t_c} \quad \text{or} \quad T=\frac{t-t_c}{(q''H/k)} \tag{1}$$

Introducing the dimensionless streamfunction ψ

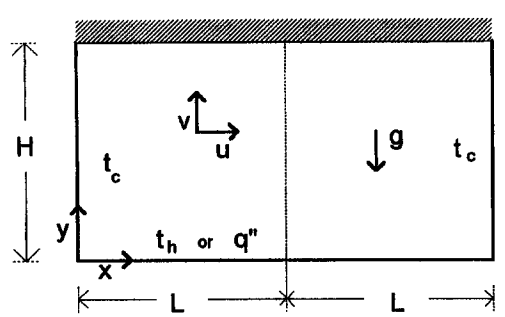

Fig. 1. Coordinate system of the cavity.

$$U=\frac{\partial\psi}{\partial Y} \quad V=-\frac{\partial\psi}{\partial X} \tag{2}$$

and the dimensionless vorticity

$$\xi=\frac{\partial V}{\partial X}-\frac{\partial U}{\partial Y} \tag{3}$$

the conservation equations for mass, momentum and energy for steady state can be written in streamfunction–vorticity form as

$$\frac{1}{Pr}\left(U\frac{\partial\xi}{\partial X}+V\frac{\partial\xi}{\partial Y}\right)=\nabla^2\xi+Ra\frac{\partial T}{\partial X} \tag{4}$$

$$U\frac{\partial T}{\partial X}+V\frac{\partial T}{\partial Y}=\nabla^2 T \tag{5}$$

$$\nabla^2\psi=-\xi \tag{6}$$

where Pr and Ra are the Prandtl number and the Rayleigh number based on the enclosure height, respectively.

The corresponding boundary conditions are

$$T=0 \quad \psi=\frac{\partial\psi}{\partial X}=0 \quad \text{at } X=0$$
$$\frac{\partial T}{\partial X}=0 \quad \psi=\xi=0 \quad \text{at } X=L/H$$
$$T=1 \quad \text{or} \quad \frac{\partial T}{\partial Y}=-1 \quad \psi=\frac{\partial\psi}{\partial Y}=0 \quad \text{at } Y=0$$
$$\frac{\partial T}{\partial Y}=0 \quad \psi=\frac{\partial\psi}{\partial Y}=0 \quad \text{at } Y=1. \tag{7}$$

It may be observed that in the boundary condition at $Y = 0$, for the case of uniform heat flux, the derivative is negative because the heat flows towards the cavity.

NUMERICAL PROCEDURE

The numerical method adopted is based on the discretization scheme proposed by Allen and Southwell [5]. Equations (4)–(6) are discretized and solved in a line-by-line basis for each step of the iterative process. The vorticity boundary value at the wall is calculated using a second-order form due to Jensen [6] and the Poisson equation (6) is discretized by the usual central-difference scheme. An under-relaxation coefficient of 0.7 for the vorticity transport equation is used in order to avoid divergence. The iterative process starts from an arbitrary vorticity field, the streamfunction is found from equation (6) and the velocity field and the vorticity at the walls are calculated. The energy equation is solved and the vorticity discretized equation coefficients calculated with the corresponding residual being determined. This residual together with the ratio

$$\sum_{i,j} \frac{|\phi_{i,j}^{n+1} - \phi_{i,j}^{n}|}{|\phi_{i,j}^{n+1}|} \leqslant 10^{-5} \tag{8}$$

where ϕ is either T or ξ, and n represents the iteration order, are used as a double checking for the convergence iterative process. If this criterion is not satisfied the vorticity discretized equation is solved and the streamfunction is found, continuing the iterative process.

The Nusselt number is calculated from the temperature field obtained at the end of the iterative process. For the case of uniform wall temperature at the cavity floor, the Nusselt number can be defined as

$$Nu = \frac{Q}{k(t_h - t_c)} \tag{9}$$

with

$$Q = \int_0^H k\left(\frac{\partial t}{\partial x}\right)_{x=0} \mathrm{d}y = -\int_0^L \left(\frac{\partial t}{\partial y}\right)_{y=0} \mathrm{d}x. \tag{10}$$

When a uniform heat flux is specified at the cavity floor, the Nusselt number is given by

$$Nu = \frac{q''L}{k(\bar{t}_h - t_c)} \tag{11}$$

where $\bar{t}_h$ is the average temperature at the cavity floor, expressed as

$$\bar{t}_h = \frac{1}{L}\int_0^L t_{(x,0)}\,\mathrm{d}x. \tag{12}$$

The temperature derivatives are evaluated by using two interior points. The integrals are approximated by the trapezoidal rule.

Although the temperature discontinuity at the intersection of the two walls at different temperatures has no influence on the numerical calculation of the interior temperatures and the flow field, it is necessary to make some considerations about this singular point in order to specify the conditions under which the values of the Nusselt number were evaluated for the case of uniform temperature at the cavity floor. As was well demonstrated by Nansteel *et al.* [7] the heat flux exhibits a non-integrable singularity at this point and consequently the overall heat transfer rate Q is unbounded. It follows that the numerical heat transfer results will be larger and larger as the grid is refined. One way to avoid this grid dependence is to introduce a well-defined temperature distribution for the transition from the temperature of one wall to the temperature of the other in the region of the bottom left corner. This procedure introduces new parameters in the studied problem and, in an engineering application, it will depend on the configuration under study.

Some authors adopted the simplest, but grid-dependent, procedure of assuming the average temperature of the two walls at the corner and keeping the adjacent nodes with the respective wall temperatures. Tests were performed to determine the grid dependence of the Nusselt number when this procedure is adopted for the studied problem. A linear temperature profile between the corner node and the next adjacent node was assumed. Figure 2 shows the results of these tests for $Ra = 10^6$, $Pr = 7.0$ and for $Ra = 10^4$, $Pr = 0.7$. The Nusselt number was evaluated along the x- and y-axes, according to equation (9). It may be seen that the grid dependence is more accentuated for $Ra = 10^4$ than for $Ra = 10^6$. For $Ra = 10^6$ when the mesh is refined from 61×61 to 91×91 grid points the increase in the Nusselt number is less than 0.1% while for $Ra = 10^4$ and the same grid refinement the increase in the Nusselt number is 5.8%. For low values of the

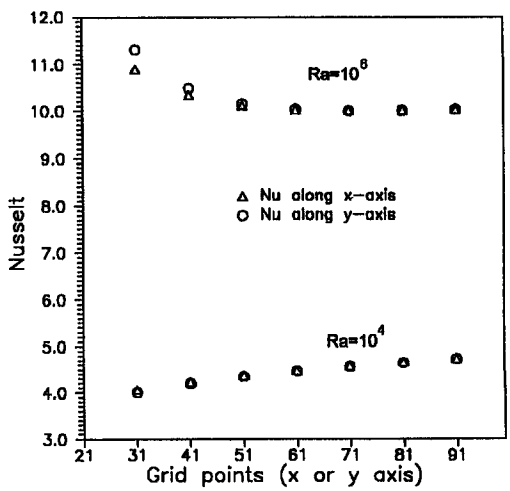

Fig. 2. The effect of the number of grid nodes on the Nusselt number for $L/H = 1$ and specified temperature at the floor: $Ra = 10^6$, $Pr = 7.0$ and $Ra = 10^4$, $Pr = 0.7$.

Rayleigh number the isotherms are closer to the conduction limit and the influence of the corner point on the overall heat transfer rate is stronger. When the Rayleigh number increases this influence diminishes becoming important only for very fine meshes. Other tests were carried out and confirmed this statement. The influence of the grid refinement on the maximum value of the streamfunction was also investigated and an increase from 61×61 to 91×91 nodal points resulted in a variation in the value of Ψ_{max} of only 0.6% for $Ra = 10^6$, $Pr = 7.0$. For $Ra = 10^4$, $Pr = 0.7$ practically no variation was observed for the same grid refinement. In view of these results it was decided to use a uniform grid with 61×61 points for all cases where $L/H = 1$ and the temperature at the intersection of the two walls was assumed as the average temperature of the two walls, keeping in mind the limitations of this procedure and remembering that better assumptions about this point depend on the specific engineering application under study.

For the shallow cavity, $L/H > 1$, an irregular grid was adopted in the x-direction to refine the cavity extremes. The procedure consists of transforming the independent variables so that in the transformed coordinate system the new domain can be covered by a grid uniformly spaced in both directions [8]. A new variable is defined for the transformed plane in the x-direction while in the y-direction the same 61 uniform grid points of the square cavity are maintained. The hyperbolic sine was used for the variable transformation, because this function is easy to derive and it permits a localized refinement.

Uniform and non-uniform grids were compared and as a general procedure, taking a uniform grid with $\Delta X = \Delta Y$ and 61 points in the y-direction as the reference, the utilization of a non-uniform grid with about one-third of the number of grid points in the x-direction produces approximately the same results as the former reference uniform grid with less computer time. For example, for $Ra = 10^6$, $L/H = 7$, $Pr = 0.7$ and uniform temperature at the floor, the difference between the values of the Nusselt number calculated for a uniform grid of 421 points in the x-direction and for a non-uniform grid of 151 points in the same direction is less than 0.7%, while the computing time is 10 times greater for the uniform grid.

Non-uniform grids of 191, 151 and 111 points in the x-direction were adopted for $L/H = 9$; 7 and 5, respectively. For $L/H = 2$ and 3 uniform grids with 61 points in the y-direction and $\Delta X = \Delta Y$ were adopted.

THE SQUARE CAVITY

The square cavity is an important starting point in the study of the flow and heat transfer in enclosures. References with configurations closest to the present work deal with this type of cavity [2–4].

The analysis is based on numerical results obtained for values of the Rayleigh number in the range 10^3–10^8 and values of the Prandtl number of 0.7 and 7.0.

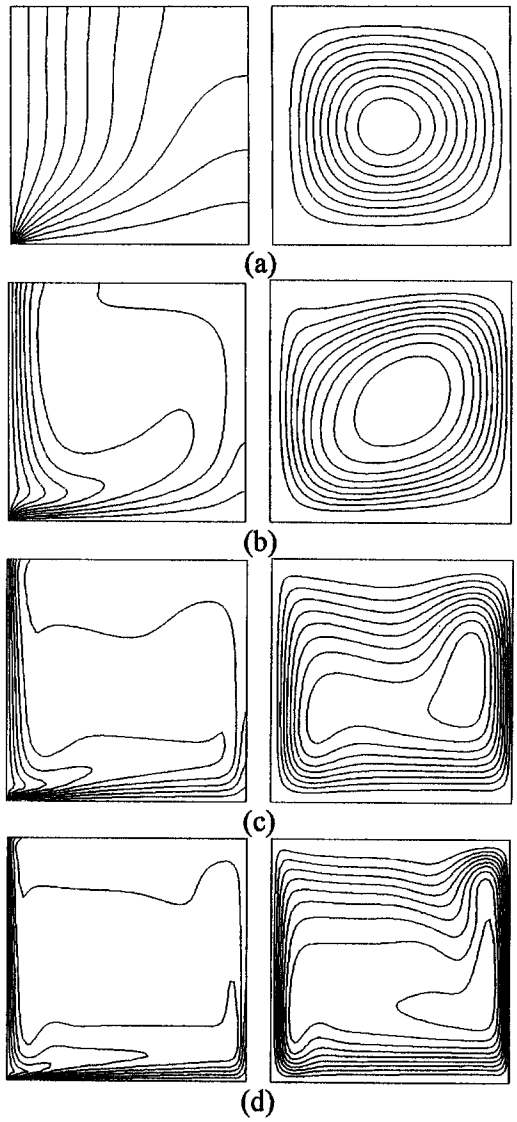

Fig. 3. Isotherms and streamlines for $Pr = 7.0$ and uniform temperature at the cavity floor. (a) $Ra = 10^3$, $\psi_{max} = 1.09$; (b) $Ra = 10^5$, $\psi_{max} = 19.16$; (c) $Ra = 10^6$, $\psi_{max} = 43.35$; (d) $Ra = 10^7$, $\psi_{max} = 75.96$.

Boundary conditions of first and second kind are considered at the cavity floor while the remaining boundaries are kept unalterated. Figure 3 illustrates the isotherms and the streamlines for uniform wall temperature at the cavity floor with $Pr = 7.0$. These contours were plotted for nine equally spaced values between zero and unity for T and between zero and Ψ_{max} for the streamfunction (values indicated in the figure captions). Initially, when $Ra = 10^4$ [Fig. 3(a)], the isotherms are closer to the diagonally symmetric temperature distribution that corresponds to the limit of pure conduction. As the value of the Rayleigh number increases, and consequently the circulation inside the cavity, the warmer fluid tends to occupy the upper right quadrant, compressing the isotherms near the

cooled vertical wall and near the heated floor. This horizontal heated layer remains attached to the cavity floor although the density stratification in this layer is unstable.

For increasing values of the Rayleigh number the temperature tends to be more uniform in the upper right region of the cavity, with higher temperature gradients near the heated cooled wall, thus suggesting the development of thermal boundary layers at these walls.

A scale analysis similar to that usually conducted for a natural convection boundary layer on a vertical wall exposed to an infinite medium [9] was applied to this study. Provided that the cavity in not tall, that is $H \leqslant L$, it may be assumed that a thermal boundary layer exists throughout the height H of the cavity cooled wall. For fluids having values of the Prandtl number of order one or greater it can be shown that the vertical thermal boundary layer thickness δ_t and the vertical velocity scale v are

$$\delta_t \cong H\,Ra^{-1/4} \tag{13}$$

$$v \cong (\alpha/H)Ra^{1/2} \tag{14}$$

The maximum value of the streamfunction Ψ_{max} is of the order of $v\delta$, where δ is the hydrodynamic boundary layer thickness near the cooled vertical wall. For the case of $Pr \geqslant 1$ fluids $\delta \cong \delta_t\, Pr^{1/2}$: therefore

$$\psi_{max} \cong Pr^{1/2}\, Ra^{1/4} \tag{15}$$

Given the order of magnitude of the cooled wall heat flow rate as $Q \cong kH(\Delta t/\delta_t)$, the order of the Nusselt number can be expressed as

$$Nu \cong \frac{Q}{k\Delta t} \cong Ra^{1/4}. \tag{16}$$

When the heat flux is specified at the cavity floor, the order of magnitude of the temperature difference must be determined. Since the total heat flow rate $q''L$ entering the cavity floor of length L should match that exiting the cooled vertical wall of height H, it follows that $\Delta t \cong (q''\delta_t/k)(L/H)$. Thus, for uniform heat flux at the cavity floor, the scales are

$$\delta_t \cong H(L/H)^{-1/5}\, Ra^{-1/5} \tag{17}$$

$$v \cong (\alpha/H)(L/H)^{2/5}\, Ra^{2/5} \tag{18}$$

$$\psi_{max} \cong \alpha(L/H)^{1/5}\, Pr^{1/2}\, Ra^{1/5} \tag{19}$$

$$Nu \cong (L/H)^{1/5}\, Ra^{1/5} \tag{20}$$

and here the Rayleigh number is based on the heat flux. Observing that $\delta_t \ll H$, the constraints on the parametric domain in which the scaling results are valid can be determined. For uniform floor temperature

$$Ra^{1/4} \gg 1 \tag{21}$$

and for uniform heat flux at the cavity floor

$$(L/H)^{1/5}\, Ra^{1/5} \gg 1. \tag{22}$$

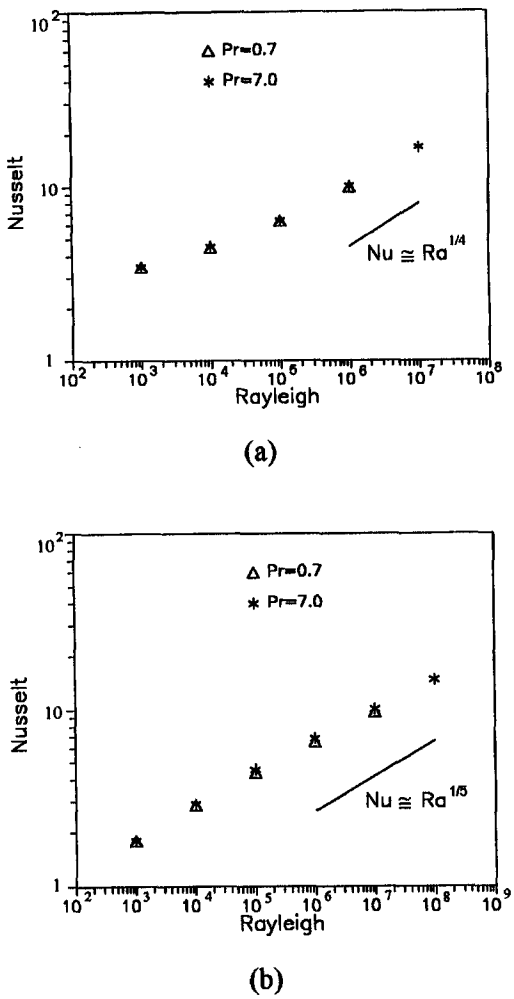

Fig. 4. Nusselt number as a function of the Rayleigh number. (a) Uniform temperature at the cavity floor; (b) uniform heat flux at the floor.

These relations represent the criterion necessary for the existence of a thermal boundary layer along the vertical wall.

Numerical results were obtained in order to verify the validity of the predicted scaling laws. Figure 4 shows values of the Nusselt number as a function of the Rayleigh number. When the temperature is specified at the cavity floor [Fig. 4(a)], the power law $Nu \cong Ra^{1/4}$ is observed more precisely only when $Ra \geqslant 10^5$, according to equation (21). For specified heat flux [Fig. 4(b)] the relation $Nu \cong Ra^{1/5}$ is satisfied in almost all the range $10^3 < Ra < 10^8$.

In both cases, for values of the Prandtl number of 0.7 and 7.0, little influence of the Prandtl number on the Nusselt number is noticed. The power laws obtained from scale analysis were also observed for ψ_{max} and v, specially for $Ra > 10^5$, as suggested by criteria (21) and (22).

The power laws presented here do not apply to the corner heated by the side and cooled from below studied by Kimura and Bejan [2]. In that case, the

vertical boundary layer does not extend along the whole height H of the heated wall, being restricted to the region near the cooled floor, where the temperature difference between the wall and the fluid is more pronounced. The stabilizing vertical temperature gradient, imposed by the cooled floor, causes a smaller circulation intensity inside the cavity and a smaller value of the Nusselt number as compared to the situation of the cavity analyzed in this work. The reduction of the circulation inside the cavity when a stabilizing vertical temperature gradient imposed was observed by Ostrach and Raghavan [10] for the classical cavity heated in one side and cooled in the opposite side.

THE SHALLOW CAVITY

Uniform wall temperature at the cavity floor

Cavity aspect ratios $L/H = 2$, 3, 5, 7 and 9 are considered here and results presented for $Pr = 0.7$ only because the influence of the Prandtl number was found to have little influence on fundamental parameters like the Nusselt number and the maximum streamfunction value.

Figure 5 shows isotherms and streamlines for $L/H = 7$ and $Ra = 10^4$, 10^5 and 10^6. It may be noticed that the flow consists of a single cell that rotates counterclockwise. This cell, when compared to the square cavity $L/H = 1$, does not occupy uniformly the whole cavity length, specially for smaller values of the Rayleigh number and higher L/H ratios. The presence of small recirculations in these cases will be discussed later in this study. As the Rayleigh number increases, the flow tends to occupy more uniformly the whole cavity, as the center of the cell moves steadily towards the cavity symmetry plane $X = L/H$. The isotherms, however, do not reach the cavity right side not even for $Ra = 10^6$. The velocity diminishes towards the cavity symmetry line (except for $Ra = 10^6$) and the cavity is approximately isothermal at this location. From this observation a thermal penetration length l can be defined, which represents the distance from $X = 0$ that is affected by the presence of the cooled wall. This penetration parameter has been used by Poulikakos [11] and Kimura and Bejan [12].

The thermal penetration length will be evaluated, for comparison purposes, as the distance between the cooled wall ($X = 0$) to the farthest point on the last isotherm drawn ($T = 0.9$). This consideration is valid when the last isotherm is not deformed by the proximity to the cavity symmetry plane. The thermal penetration as defined above is illustrated in Fig. 6(a) for $Ra = 10^5$ and $L/H = 5$, 7 and 9. It can be seen that the isotherm contours are no longer affected by the cavity length. The same happens to the streamlines, as shown in Fig. 6(b), except for a little distortion at the cavity symmetry for $L/H = 5$. The independence of the thermal penetration length respective to the cavity aspect ratio L/H suggests that this length should be a function of the Rayleigh number only. It is supposed that practically all the heat transfer from the cavity floor takes place along the region of the penetration length. The heat flow rate lost at the cooled vertical wall must balance the heat input through the floor. In scale analysis this results in

$$kH\Delta t/\delta_t \cong kl\Delta t/H. \tag{23}$$

Substituting the value of the thermal boundary layer thickness δ_t from equation (13) yields

$$l \cong H\,Ra^{1/4}. \tag{24}$$

This power law can be verified in Fig. 7 for $Ra \geqslant 10^4$ and $L/H = 5$, 7 and 9. Regardless of the ratio L/H, the results are almost coincidents for the same value of the Rayleigh number. When $Ra = 10^3$ the isotherms are less deformed in relation to the diagonally symmetric limit of pure conduction, and the temperature gradients near the cooled vertical wall are relatively smooth. For this situation a boundary layer flow structure adjacent to the vertical wall is not well established and the penetration length does not obey the power law of equation (24).

The influence of the cavity aspect ratio L/H on the Nusselt number is shown in Fig. 8, for $Ra = 10^3$–10^6. It can be seen that the effect of the ratio L/H on the Nusselt number increases with the Rayleigh number. For $Ra = 10^3$–10^4 the value of the Nusselt number varies very little with the ratio L/H. By observing the curve for $Ra = 10^6$, it may be noticed that the increase in the Nusselt number tends to stabilize for $L/H > 5$. For $L/H \leqslant 5$, the cavity is thermally active along its whole length L. When the cavity length is increased from $L/H = 1$ up to $L/H = 5$ the horizontal jet of cooled fluid is in contact with a larger dimension of the cavity floor, thus increasing the overall heat transfer rate to the fluid. For $L/H = 7$ and 9 the thermal penetration is incomplete and the region farther from the cooled wall is thermally inactive and does not contribute to the increase in the Nusselt number. It is worth mentioning that for $L/H = 7$ and 9 the values of the Nusselt number for the cavity approaches the value of the Nusselt number for an isothermal vertical wall in an infinite medium. The thermally inactive region, present in shallower cavities, acts approximately as an isothermal fluid reservoir.

The flow remains unicellular, independently of the ratio L/H and the Rayleigh number. Note that the heated layer adjacent to the cavity floor remains attached over the entire horizontal span of the enclosure, although the density stratification in this layer is unstable due to the fluid flowing vertically downward along the cold wall, as a consequence of the pressure gradient caused by the heated fluid that fills the upper part of the cavity and returns to the cooled wall. For $L/H = 9$ and $Ra = 10^4$ and 10^5, small recirculations were observed near the cavity symmetry at $X = L/H$. These recirculations are of very low intensity, of the order of 1–2.5% of ψ_{max}, and occur in a region practically isothermal for lower values of the Rayleigh number and long horizontal cavities, being

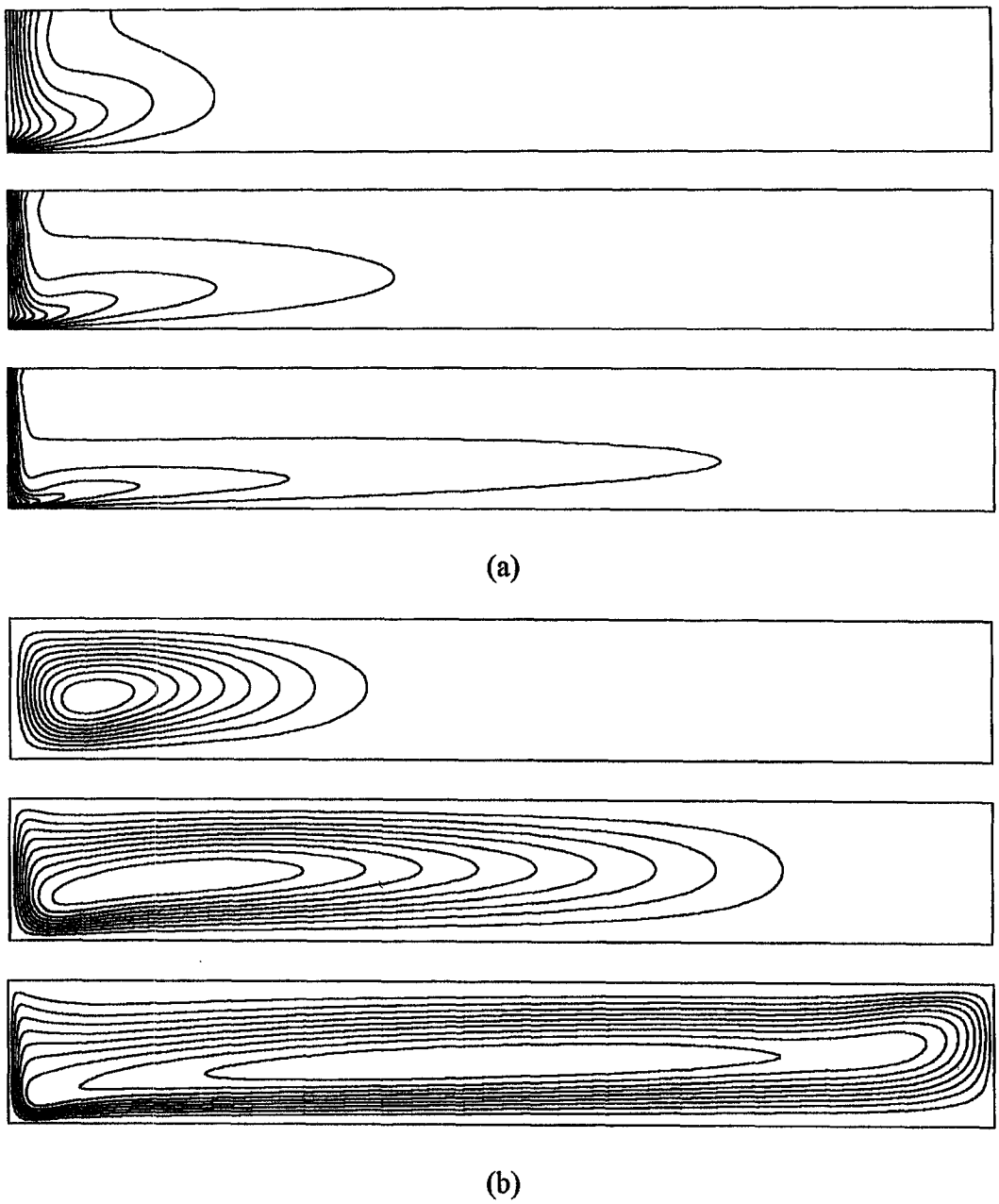

Fig. 5. Isotherms and streamlines for $L/H = 7$ and uniform wall temperature at the cavity floor for $Ra = 10^4$, 10^5 and 10^6. (a) Isotherms; (b) streamlines ($\psi_{max} = 6.67$, 16.46 and 39.49).

caused by the viscous drag produced by the periphery flow of the main cell. Therefore they do not consist of a convective effect due to an unstable vertical temperature gradient.

Uniform heat flux at the cavity floor

For the case of a specified constant heat flux at the cavity floor the presence of a heat flux along the entire floor length makes the cavity completely thermally active.

Figure 9 shows the results for $L/H = 7$ and $Ra = 10^3$, 10^5 and 10^6. The flow pattern, as before, consists of a counterclockwise cell. However in this case the cell fills the cavity in all its extension. It may be noticed that, for all cases, the center of the cell migrates from left to right when the Rayleigh number increases, a tendency also observed for uniform temperature though in a less pronounced way. For the isotherms, the temperature gradient increases monotonically in the x-direction. This is more uniformly distributed along the cavity for $Ra = 10^3$ and 10^4, although it is always more intense near the cooled wall because it is in this wall that all the heat supplied along the cavity floor has to be removed. With the

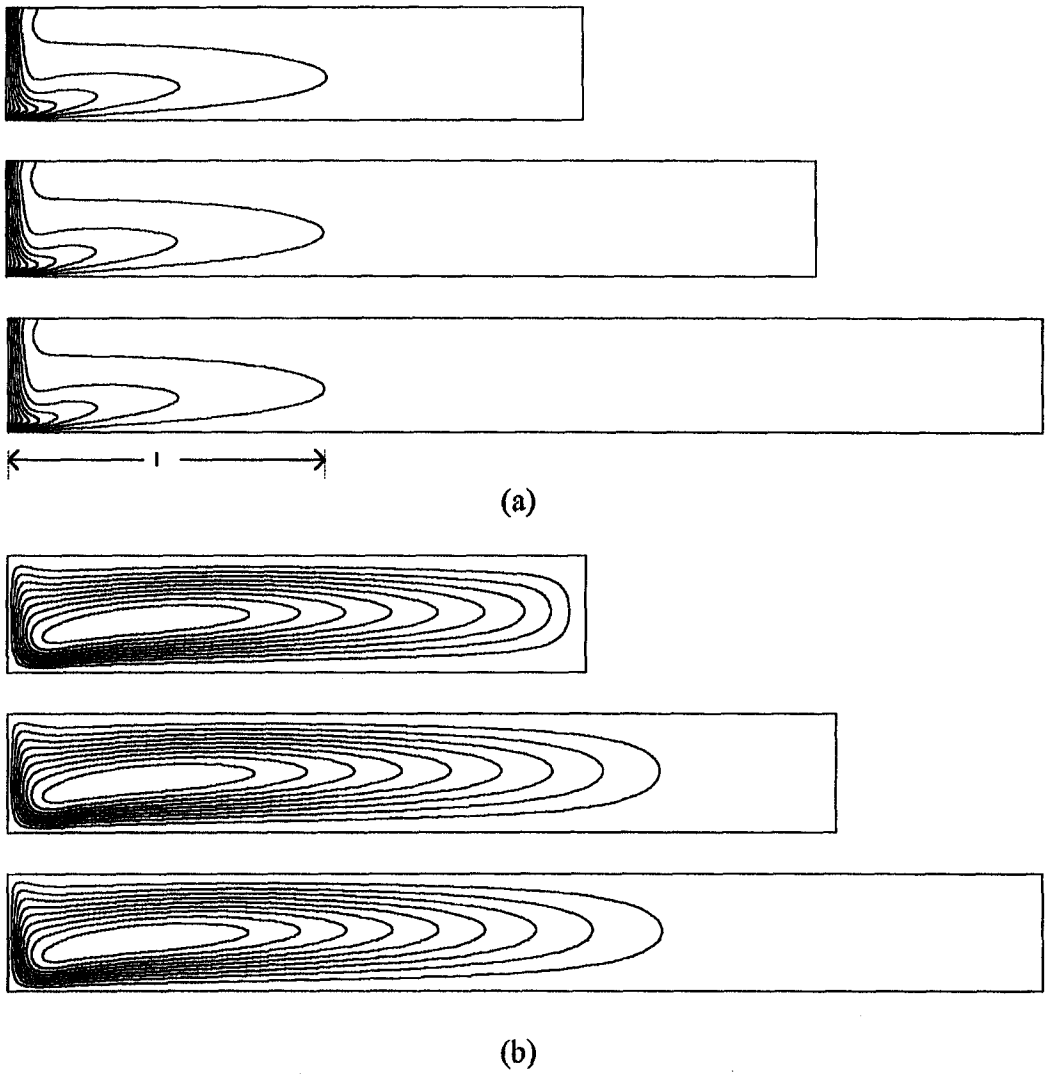

Fig. 6. Illustration of the thermal penetration length l for $Ra = 10^5$ and for $L/H = 5$, 7 and 9. (a) Isotherms; (b) streamlines ($\psi_{max} = 16.48$, 16.46 and 16.45).

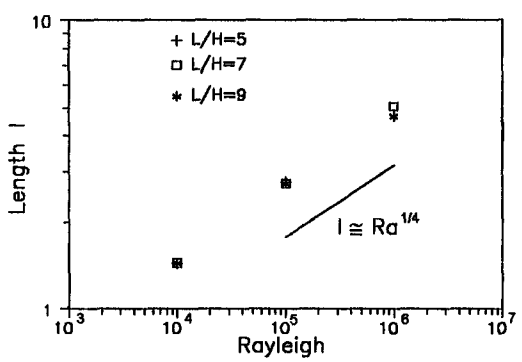

Fig. 7. Thermal penetration length vs Rayleigh number.

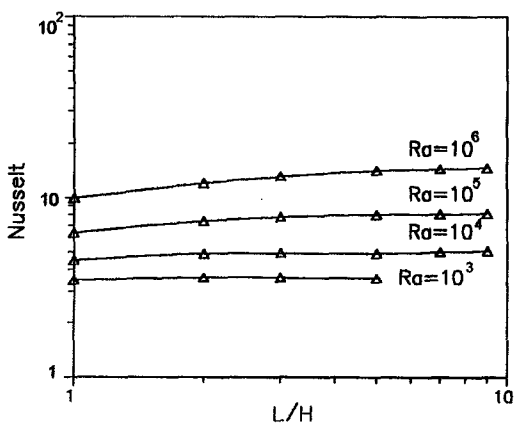

Fig. 8. Nusselt number as a function of the aspect ratio L/H.

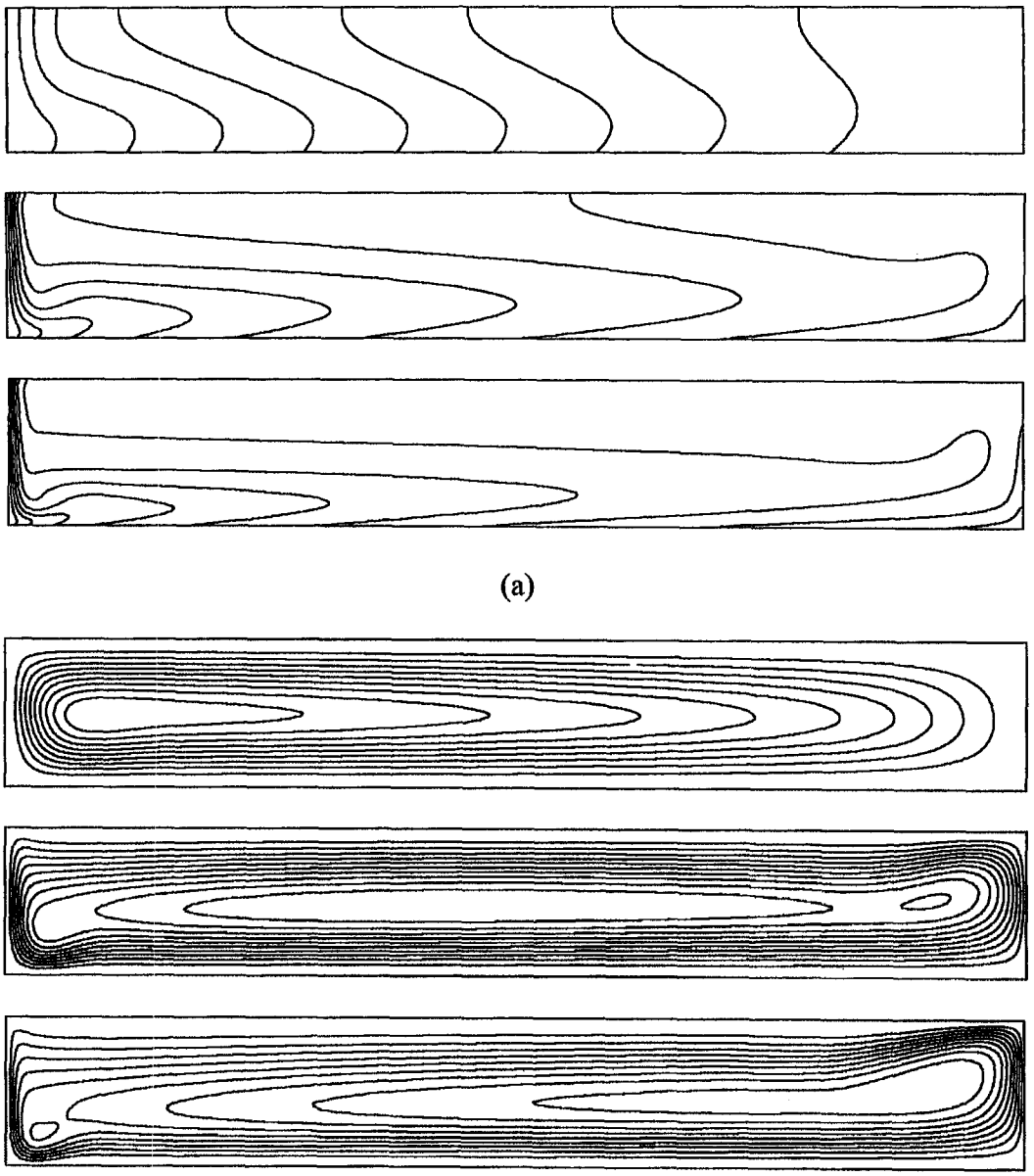

Fig. 9. Isotherms and streamlines for $L/H = 7$ and uniform heat flux at the cavity floor for $Ra = 10^3$, 10^5 and 10^6. (a) Isotherms; (b) streamlines ($\psi_{max} = 3.46$, 16.53 and 38.55).

increase of the Rayleigh number, and consequently the increase of the circulation, the heated fluid returning after changing its direction at the symmetry line tends to fill the upper part of the cavity enhancing the temperature gradient near the cooled wall, as can be noticed by the compression of the isotherms in this region. The pressure due to the flow, induced in the upper part by buoyancy and by the upward jet, compresses the fluid that flows in the lower part of the cavity. This effect contributes to the stabilization of the fluid layer adjacent to the heated cavity floor where the vertical temperature gradient is unstable.

The influence of the Rayleigh number and of the ratio L/H on the Nusselt number is shown in Fig. 10. The power law $Nu \cong Ra^{1/5}$ is better observed for $Ra \geqslant 10^5$, irrespective of the ratio L/H. As for the Nusselt number as a function of the aspect ratio L/H, when this ratio increases, the Nusselt number decreases for $Ra = 10^3$, is almost invariant for $Ra = 10^4$ and increases for $Ra > 10^4$. This behavior can be understood by analyzing the Nusselt number in a limit situation when the Rayleigh number tends to zero. The heat transfer in this case approaches that of pure conduction limit, illustrated in Fig. 10(b) as a

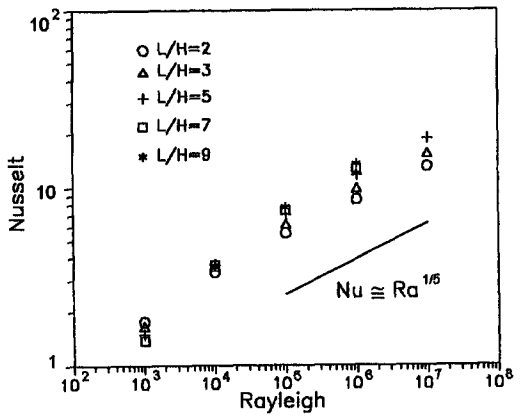

(a)

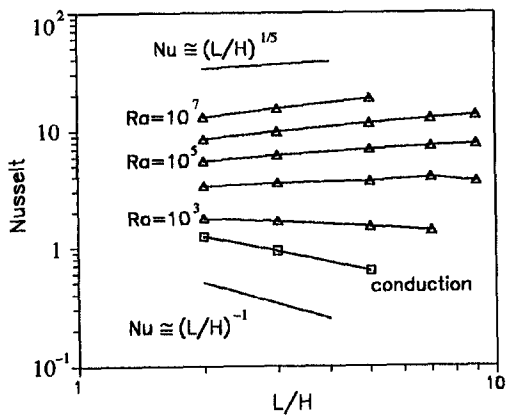

(b)

Fig. 10. The Nusselt number as a function of: (a) Rayleigh number, (b) aspect ratio.

reference. When the Rayleigh number is small the isotherms fill the cavity in a relatively uniform way. Therefore the cavity length L can be taken as the characteristic dimension of the region where the temperature variation along the x-axis are taking place. Thus, the total heat flow rate across the cavity can be written as

$$Q \cong kH\frac{\Delta t}{L} \tag{25}$$

which results, using the definition of the Nusselt number, in

$$Nu \cong (L/H)^{-1}. \tag{26}$$

It may be noticed how the Nusselt number for pure conduction in Fig. 10(b) varies in a way very close to that predicted by equation (26). The Nusselt number variation with the ratio L/H falls gradually between the limits of the power laws given by equations (20) and (26).

The variation of the maximum streamfunction value with the Rayleigh number was observed to be in good agreement with the power law given by equation (19) for $Ra = 10^6$–10^7. The variation with L/H was also in accordance with equation (19), specially for $L/H \geqslant 5$ and $Ra > 10^4$. These observations agree with what was suggested in equation (22) for the range of validity of the scale analysis for uniform heat flux at the cavity floor.

Recirculations were not observed for shallow cavities with uniform heat flux at the floor, because in this case isothermal regions are not present. The occurrence of a clockwise secondary cell is prevented by the monotonically increasing temperature gradient along the x-axis.

CONCLUSIONS

In this article, the phenomenon of natural convection heat transfer in rectangular enclosures heated from below and symmetrically cooled from the sides has been studied numerically for a range of values of the relevant parameters of the problem like the Rayleigh number and the aspect ratio L/H. The results showed a little influence of the Prandtl number on the heat transfer and on the flow circulation inside the cavity.

For the square cavity $L/H = 1$ the boundary condition at the cavity floor, uniform surface temperature or uniform heat flux, does not strongly affect the flow or the isotherm contours. For a shallow cavity, however, there are markedly differences when the surface temperature or the heat flux is prescribed. In the case of uniform temperature at the cavity floor, the cavity is not always thermally active along its whole extension and the flow does not fill it uniformly in these cases. When the heat flux is prescribed, the isotherms and the streamlines occupy more uniformly the whole cavity, even for low values of the Rayleigh number.

The flow structure was found to consist of a single counterclockwise cell for all cases studied, except for a small secondary cell due to viscous drag observed in some cases for uniform temperature at the cavity floor.

A scale analysis similar to that conducted for a natural convection boundary layer on a vertical wall exposed to an infinite medium predicted the basic flow features in the boundary layer regime. The heated cavity floor receives the cooled fluid and warms it, allowing the fluid to perform a cycle that approaches to what happens in a cooled vertical wall exposed to an infinite medium.

REFERENCES

1. S. Ostrach, Natural convection in enclosures, *J. Heat Transfer* **110**, 1175–1190 (1988).
2. S. Kimura and A. Bejan, Natural convection in a differentially heated corner region, *Phys. Fluids* **28**(10), 2980–2989 (1985).
3. R. Anderson and G. Lauriat, The horizontal natural convection boundary layer regime in a closed cavity, *Proceedings of the Eighth International Heat Transfer*

Conference Vol. 4, pp. 1453–1458, San Francisco, CA (1986).
4. M. November and M. W. Nansteel, Natural convection in rectangular enclosures heated from below and cooled along one side, *Int. J. Heat Mass Transfer* **30,** 2433–2440 (1987).
5. D. N. de Allen and R. V. Southwell, Relaxation methods applied to determine the motion, in two dimensions, of a viscous fluid past a fixed cylinder, *Q. J. Mech. Appl. Math.* **8,** 129–145 (1955).
6. V. G. Jensen, Viscous flow round a sphere at low Reynolds number (40), *Proc. R. Soc. Lond. Ser. A* **249,** 346–366 (1959).
7. M. Nansteel, S. Sadhal and P. Ayyaswamy, Discontinuous boundary temperatures in heat transfer theory, Session on Significant Questions in Buoyancy Affected Enclosure or Cavity Flows, ASME Winter Annual Meeting, December (1986).
8. D. A. Anderson, J. C. Tannehill and R. H. Pletcher, *Computational Fluid Mechanics and Heat Transfer.* Hemisphere New York (1984).
9. A. Bejan, *Convection Heat Transfer.* John Wiley, New York (1984).
10. S. Ostrach and C. Raghavan, Effect of stabilizing thermal gradients on natural convection in rectangular enclosures, *J. Heat Transfer* **101,** 238–243 (1979).
11. D. Poulikakos, Natural convection in a confined fluid-filled space driven by a single vertical wall with warm and cold regions, *J. Heat Transfer* **107,** 867–876 (1985).
12. A. Bejan and S. Kimura, Penetration of free convection into a lateral cavity, *J. Fluid Mech.* **103,** 465–478 (1981).